Environ. Sci. Technol. **2007**, *41,* 4389−4396

Mechanistic Studies of the Photocatalytic Degradation of Methyl Green: An Investigation of Products of the Decomposition Processes

CHIING-CHANG CHEN* AND CHUNG-SHIN LU

Department of General Education, National Taichung Nursing College, Taichung 403, Taiwan, ROC

The methyl green (MG) dye dissolves into an alkaline solution when the pH value is too high (pH 9). The cationic MG dye molecules are converted into the colorless carbinol base (CB) and produce crystal violet (CV) dye and ethanol by hydroxide anion. Thirty-three intermediates of the process were separated, identified, and characterized by HPLC-ESI-MS technique in this study and their evolution during the photocatalytic reaction is presented. Moreover, the other intermediates formed in the photocatalytic degradation MG processes were separated and identified by HPLC-PDA technique. The results indicated that the *N*-de-methylated degradation of CV dye took place in a stepwise manner to yield *N*-de-methylated CV species, and the *N*-de-alkylated degradation of CB also took place in a stepwise manner to yield *N*-de-alkylated CB species generated during the processes. Moreover, the oxidative degradation of the CV dye (or CB) occurs to yield 4-(*N*,*N*-dimethylamino)phenol (DAP), 4-(*N*,*N*-dimethylamino)-4′-(*N*′,*N*′-dimethylamino)benzophenone (DDBP) and their *N*-de-methylated products [or to yield 4-(*N*-ethyl-*N*,*N*-dimethyl)aminophenol (EDAP), DDBP, 4-(*N*-ethyl-*N*,*N*-dimethylamino)-4′-(*N*′,*N*′-dimethylamino)benzophenone (EDDBP), DAP, and their *N*-de-alkylated products], which were found for the first time. A proposed degradation pathway of CV and CB is presented, involving mainly the *N*-de-alkylation and oxidation reaction.

1. Introduction

The semiconductor TiO_2 is broadly used as a photocatalyst because of its nontoxicity, photochemical stability, and low cost (*1*, *2*). It is has proven to be an excellent photocatalyst material, on which many organic substrates have been shown to be oxidatively degraded and ultimately mineralized completely (*3*−*5*). Studies on the photocatalytic degradation of different classes of organics have appeared in the literature, and most of them include a detailed examination of the so-called primary processes under different working conditions (*6*−*12*). However, less attention has been paid to the study of the degradation mechanism and to the identification of major transient intermediates, which have been more recently recognized as very important aspects of these processes, especially in view of their practical applications.

* Corresponding author phone: 886-4-2219-6975; fax: 886-4-2219-4990; e-mail: ccchen@ntcnc.edu.tw.

Cationic triphenylmethane dyes have found widespread use as colorants in industry and as antimicrobial agents (*13*). Recent reports indicate that they may further serve as targetable sensitizers in the photodestruction of specific cellular components or cells (*14*). MG is basic triphenylmethane-type dicationic dye, usually used for staining solutions in medicine and biology (*15*) and as a photochromophore to sensitize gelatinous films (*16*). It has been used to differentiate between deoxyribonucleic acid and ribonucleic acid (*17*). The binding of MG to DNA is probably ionic, as opposed to intercalative, and it remains so stably bound to double stranded DNA that, with its conversion to the colorless carbinol form, it has been used to assess the binding of other molecules to DNA (*18*). However, great concern has arisen about the thyroid peroxidase-catalyzed oxidation of the triphenylmethane class of dyes because the reactions might form various *N*-de-alkylated primary and secondary aromatic amines, with structures similar to aromatic amine carcinogens (*19*).

Serpone et al. (*20*−*21*) have reported that Sulforhodamine-B (an anionic triphenylmethane dye) appears to photodegrade under the TiO_2-mediated photocatalysis process in near-neutral solution via two competitive pathways: one was *N*-de-alkylation of the chromophore skeleton, which has been clearly studied, and the other was cleavage of the whole conjugated chromophore structure, which has never been studied. The mechanistic details remained uncertain.

The pH values of solution can drastically influence the structure of triphenylmethane dyes (*22*) and the surface characteristics of TiO_2 particles (*2*). The triphenylmethane dye dissolves to alkaline solution, when the pH value is too high, and the dye molecules are converted into a colorless carbinol base. The photodegradation of MG dye and its carbinol base under TiO_2-mediated photocatalysis process has not been studied. Accordingly, this study focused on the separation and identification of the photocatalytic reaction intermediates in hopes of shedding some light on the mechanistic details of photodegradation of MG dye and its carbinol base in the TiO_2/UV process as a foundation for future application of this energy saving technology.

2. Experimental Section

2.1. Chemicals. P25 TiO_2 was from Degussa, having a surface area of ca. 55 m^2g^{-1} and a measured size of the primary particles around 20−30 nm. MG dye (CI = 42590) and 4-(*N*-methylaminophenol) (MAP; with a guaranteed purity of 98%) were obtained from Aldrich. We purchased 4-aminophenol (AP; analytical standard) from Riedel-de Haen. Crystal violet (CV) was obtained from Tokyo Kasei. The 4-(*N*,*N*-dimethylamino)-4′-(*N*′,*N*′-dimethylamino)benzophenone was obtained from Acros Organics. All of them were used without any further purification. The chemical structure of the MG dye is displayed in Figure 1. Reagent-grade ammonium acetate, sodium hydroxide, nitric acid, and HPLC-grade methanol were purchased from Merck.

2.2. Instruments and Apparatus. A Waters ZQ LC/MS system, equipped with a binary pump, a photodiode array detector, an autosampler, and a micromass detector, was used for separation and identification. The C-75 Chromato-Vue cabinet of UVP provides a wide area of illumination from the 15 watt UV-365 nm tubes positioned on two sides of the cabinet interior.

2.3. Experimental Procedures. An aqueous TiO_2 dispersion was prepared by adding 50 mg of TiO_2 powder to a 100 mL solution containing the MG dye at appropriate concentrations. The concentration of MG aqueous solutions

10.1021/es062465g CCC: $37.00 © 2007 American Chemical Society
Published on Web 05/12/2007

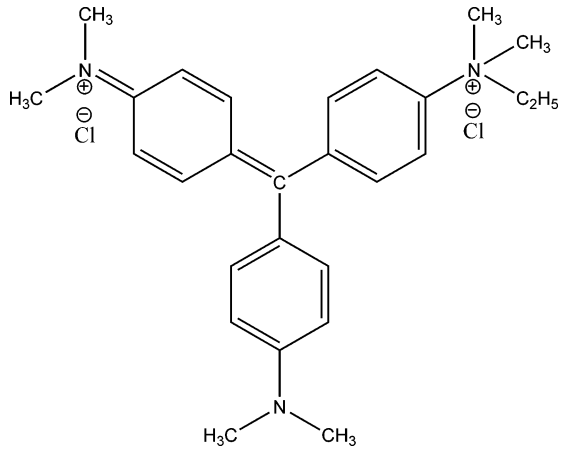

FIGURE 1. Chemical structure and formula of methyl green dye (CI = 42590): molecular formula: $C_{27}H_{35}Cl_2N_3 \cdot xZnCl_2$.

was adjusted to 0.05 g L^{-1}. For reactions in different pH media, the initial pH of the suspensions was adjusted by the addition of either NaOH or HNO_3 solutions. Prior to irradiation, the dispersions were magnetically stirred in the dark for ca. 30 min to ensure the establishment of adsorption/desorption equilibrium. Irradiations were carried out using two UV-365 nm lamps (15 W). The distance between the irradiated solution and the lamps was 14 cm. An average irradiation intensity of 5.2 W/m^2 was maintained throughout the experiments and was measured by internal radiometer. At any given irradiation time interval, the dispersion was sampled (5 mL), centrifuged, and subsequently filtered through a Millipore filter (pore size, 0.22 μm) to separate the TiO_2 particles.

After each irradiation cycle, the amount of the residual dye was determined by HPLC. The analysis of organic intermediates was accomplished by HPLC-ESI-MS after the readjustment of the chromatographic conditions to make the mobile phase compatible with the working conditions of the mass spectrometer. Solvent A was 25 mM aqueous ammonium acetate buffer (pH 6.9) while solvent B was methanol instead of ammonium acetate. LC was carried out on an Atlantis dC18 column (250 mm × 4.6 mm i.d., dp = 5 μm). The flow rate of the mobile phase was set at 1.0 mL/min. A linear gradient was set as follows: $t = 0$, $A = 95$, $B = 5$; $t = 20$, $A = 50$, $B = 50$; $t = 60$, $A = 10$, $B = 90$; $t = 65$, $A = 95$, $B = 5$. The column effluent was introduced into the ESI source of the mass spectrometer.

3. Results and Discussion

3.1. Control Experiments. To prove the role of TiO_2 in the photocatalysis reaction, three sets of experiments were performed to compare MG degradation rates with and without catalysts at pH 6. The results are presented in **Figure 2**. First, the experiment with TiO_2 only showed that a small amount of MG (about 1.4%) was adsorbed on the TiO_2 surface. Control experiments performed in the dark indicated the hydrolysis and adsorption of MG on TiO_2 particles did not affect its concentration during these experiments. Next, the results of the photolysis and photocatalytic experiments showed that the photolysis reaction resulted in a 4.7% decrease in the MG concentration after 20 h while the MG was 99.9% removed after 20 h in the case of the photocatalytic reaction. It has been reported *(23−24)* that the direct photocatalytic degradation of sulforhodamine dye in aqueous TiO_2 dispersions has been examined and compared to the photosensitization process. Under UV irradiation, the excitation of dye is negligible compared with the excitation of TiO_2. Therefore, we tentatively propose that MG photocatalytic degradation proceed by TiO_2 under UV irradiation.

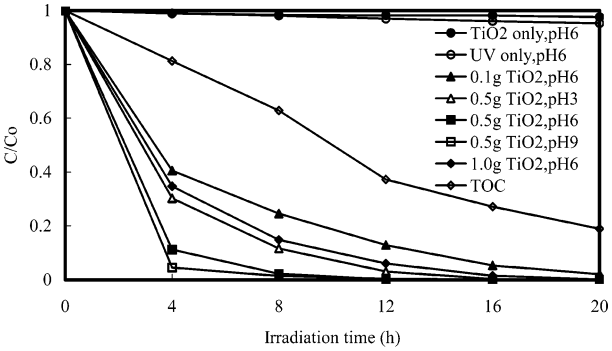

FIGURE 2. (a) MG degradation under the control conditions (TiO_2 only and UV only) and photocatalytic conditions (experimental conditions : MG = 0.05gL^{-1}, TiO_2 = 0 gL^{-1} in photolysis, 0.5 gL^{-1} in photocatalysis, UV-365 nm in photolysis and photocatalysis conditions). (b) Influence of the catalyst concentration on the photodegradation rate for the decomposition of MG. Experimental condition: dye concentration (0.05 gL^{-1}), P25 (0, 0.1, 0.5, and 1 gL^{-1}), pH 6, absorbance was recorded at 592 nm, continuous stirring, and irradiation time 20 h. (c) pH effect on the MG photodegradation rate with concentrations of TiO_2 to be 0.5 gL^{-1} and MG to be 0.05 gL^{-1}. (d) Depletion in TOC as a function of irradiation time for an aqueous solution of MG in the presence of TiO_2. Experimental condition: dye concentration (0.05 gL^{-1}), P25 (0.5 gL^{-1}), pH 6, irradiation time 20 h.

3.2. Effect of Photocatalyst Concentration. The effect of photocatalyst concentration on the photodegradation rate of the MG dye was investigated by employing different concentrations of TiO_2 ranging from 0.1 to 1.0 gL^{-1}. As expected, the photodegradation rate of the MG was found to increase, and then decrease with the increase in the catalyst concentration (Figure 2). Above 0.5 gL^{-1} of TiO_2, the initial rate of MG degradation is not affected further by a progressive increase in TiO_2 concentration. This is a general characteristic of heterogeneous photocatalyst, and our results are in agreement with earlier reports (*12*).

3.3. pH Effect. The point of zero charge (pHpzc) for TiO_2, or pH at which the surface of this oxide is uncharged, is around 6.8. Above and below this value, the catalyst is negatively or positively charged (*25*). However, the adsorption of the substrate onto the TiO_2 surface directly affects the occurrence of electron transfer between the excited dye and TiO_2 and further influences the degradation rate. The surface becomes *negatively* charged, and the number of adsorption sites may decrease above the isoelectric point of TiO_2. As shown in Figure 2, the efficiency of the photocatalytic degradation of MG depends on the initial pH of the solution used in the reaction. The photodegradation rate of the MG dye was found to increase with the increase in pH value.

3.4. Evolution of TOC. The complete mineralization of 1 mol of the MG dye molecule implies the formation of the equivalent amount (27 mol) of CO_3^{2-} at the end of the treatment. However, the formation profile of TOC (shown in Figure 2, curve TOC) clearly indicates that the reaction does not go to completion. In fact, after 20 h irradiation, only about 81.0% of the initial organic carbon has been transformed into CO_2, which implied that there still existed other organic compounds in the irradiated solution. This is supported by the HPLC-PDA analysis, which suggests the presence of residual organic products even after 20 h irradiation, confirming the noticeable degradation of the examined dye.

3.5. Separation of the Intermediates. The solution of MG dye during the degradation process with UV irradiation was examined using HPLC-PDA-ESI-MS at different irradiation times. The chromatograms at pH 9, recorded at 580, 350, 300, and 250 nm, are illustrated in Figure 3. With

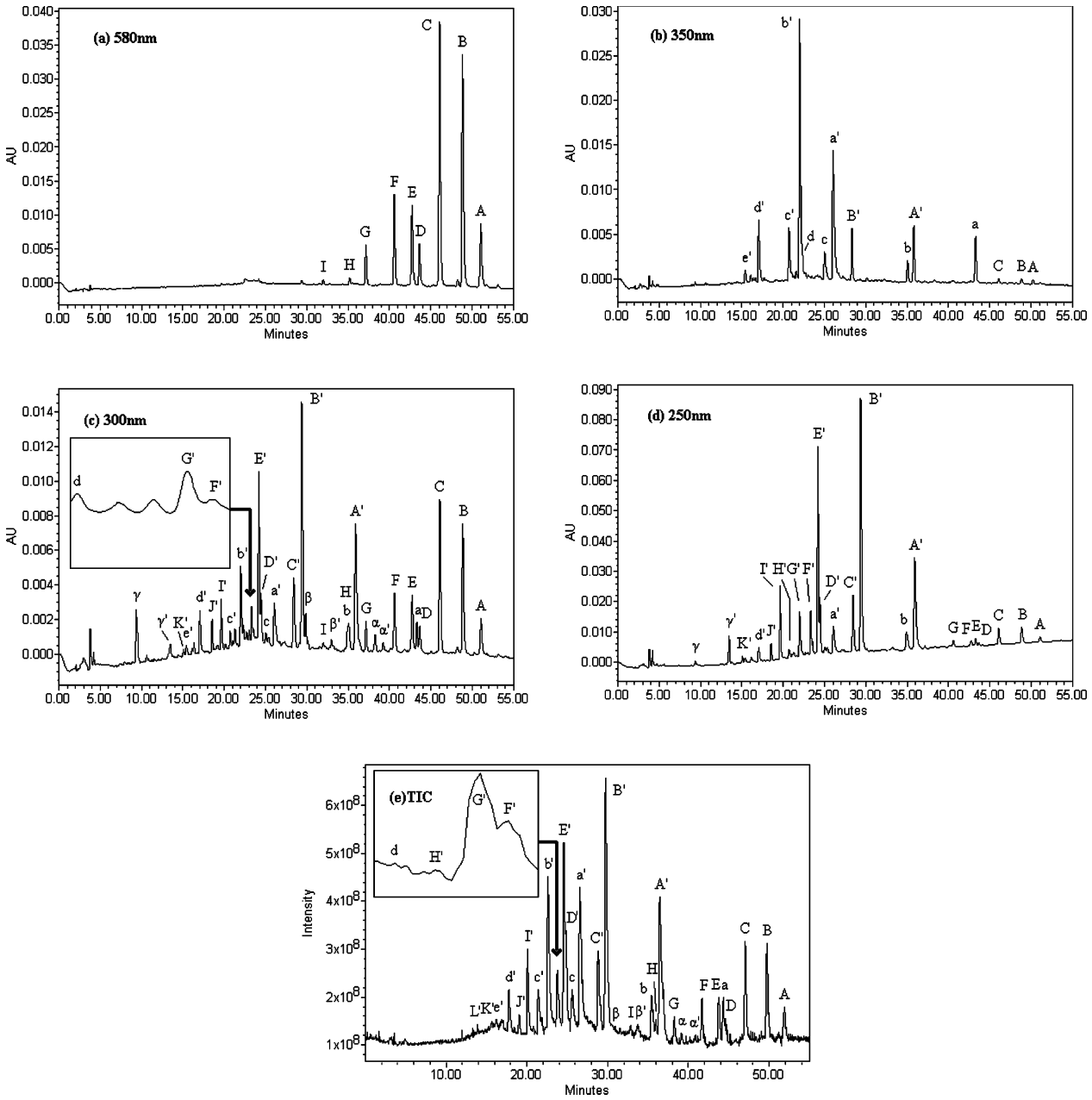

FIGURE 3. HPLC chromatogram of the intermediates, recorded at (a) 580 nm, (b) 350 nm, (c) 300 nm, (d) 250 nm, and (e) total ion chromatogram of the photodegraded intermediates with TiO_2 0.5 gL^{-1}, at pH 9, at 8 h of irradiation.

irradiation up to 8 h at pH 9, 33 components were identified, all with retention time of less than 55 min. We marked the MG dye and its related intermediates as species **A**−**I**, **a**−**d**, **a′**−**e′**, α−γ, α′−γ′, and **A′**−**K′** in the chromatograms, recorded at 580, 350, 300, and 250 nm. Except for the initial MG dye, the other peaks initially increased before subsequently decreasing, indicating formation and transformation of the intermediates.

3.6. Identification of the Intermediates. *3.6.1 UV−vis Spectra of the Intermediates.* The absorption spectra of each intermediate in the visible and ultraviolet spectral region (see Figure 4, Supporting Information) are measured corresponding to the peaks in Figure 3, respectively. From these results, several families of intermediates can be distinguished:

(1) The first family was marked in the chromatogram and is illustrated in Figure 3a, recorded at 580 nm. The absorption spectra of each intermediate in the visible spectral region around 588.1 nm are depicted in the Supporting Information (see Figure 4, Supporting Information) and correspond to the peaks **A**−**I** in Figure 3a. The intermediate has the wavelength position of its major absorption band moved toward the blue region, λ_{max}, **A**, 588.1 nm; **B,** 580.7 nm; **C**, 573.4 nm; **D**, 580.7 nm; **E**, 568.5 nm; **F**, 568.5 nm; **G**, 555.0 nm; **H**, 561.2 nm; **I**, 552.6 nm. The first family of intermediates may be the *N*-de-methylation of the CV dye.

(2) The second family was marked in the chromatogram and is illustrated in Figure 3b, recorded at 350 nm. The absorption spectra of each intermediate in the ultraviolet spectral region around 350 nm are depicted in the Supporting Information (see Figure 4, Supporting Information) and correspond to the peaks **a**−**d** and **a′**−**e′** in Figure 3b. The *N*-de-alkylation of the DDBP (EDDBP), produced by cleavage of the CV (CB), has the wavelength position of its major absorption band moved toward the blue region, λ_{max}, **a**, 365.5 nm; **b**, 362.1 nm; **c**, 361.2 nm; **d**, 344.1 nm (**a′**, 372.8 nm; **b′**, 364.3 nm; **c′**, 361.3 nm; **d′**, 345.4 nm; **e′**, 328.6 nm). The proposed intermediate (**a**) has been compared with standard material of 4-(*N*,*N*-dimethylamino)-4′-(*N*′,*N*′-dimethylami-

TABLE 1. Identified Photodegradation Products and Their Main Fragments Determined by HPLC-PDA-ESI-MS

peaks	compounds	intermediates	retention time (min)	[$M + H^+$]	ESI-MS spectrum ions (m/z)	absorption maximum (nm)
A	DDDPR; CV	*N*,*N*-dimethyl-*N*′,*N*′-dimethyl-*N*″,*N*″-di methylpararosaniline	51.90	372.13	251.22	588.1
B	DDMPR	*N*,*N*-dimethyl-*N*′,*N*′-dimethyl-*N*″-methylpararosaniline	49.71	358.17	196.71	580.7
C	DMMPR	*N*,*N*-dimethyl-*N*′-methyl-*N*″-methylpararosaniline	47.00	344.21	236.93	573.4
D	DDPR	*N*,*N*-dimethyl-*N*′,*N*′-dimethylpararosaniline	44.57	344.14	251.09; 222.91; 196.71	580.7
E	MMMPR	*N*-methyl-*N*′-methyl-*N*″-methyl pararosaniline	43.76	330.11	196.91	567.5
F	DMPR	*N*,*N*-dimethyl-*N*′-methylpararosaniline	41.70	330.11	237.06; 196.91	568.5
G	MMPR	*N*-methy-*N*′-methylpararosaniline	38.23	316.09	222.91; 208.88	555.0
H	DPR	*N*,*N*-dimethylpararosaniline	35.99	316.15	404.12; 372.13; 268.98	561.2
I	MPR	*N*-methylpararosaniline	32.84	302.25	344.08; 269.24; 196.78	552.6
A′	ED-DD−TPM; CB	[4-(*N*-ethyl-*N*,*N*-dimethylamino)][4′-(*N*′,*N*′-dimethylamino)][4″-(*N*″,*N*″-dimethylamino)]triphenylmethanol	36.43	418.27	372.13; 269.05; 241.05	259.5
B′	ED-DM−TPM	[4-(*N*-ethyl-*N*,*N*-dimethylamino)][4′-(*N*′,*N*′-dimethylamino)][4″-(*N*″-methylamino)]triphenylmethanol	29.75	404.18	358.17; 269.11; 255.02	254.8
C′	EM-DD−TPM	[4-(*N*-ethyl-*N*-methylamino)][4′-(*N*′,*N*′-dimethylamino)][4″-(*N*″,*N*″-dimethylamino)]triphenylmethanol	28.83	404.15	358.13; 269.05; 254.95	253.6
D′	D−DD−TPM	[4-(*N*,*N*-dimethylamino)][4′-(*N*′,*N*′-dimethylamino)][4″-(*N*′,*N*″-dimethylamino)]triphenylmethanol	24.84	390.09	344.14; 269.05; 240.99	248.9
E′	E-DD−TPM	[4-(*N*-ethylamino)][4′-(*N*′,*N*′-dimethylamino)][4″-(*N*″,*N*″-dimethylamino)]triphenylmethanol	24.58	390.09	344.14; 255.08	251.2
F′	EM-DM−TPM	[4-(*N*-ethyl-*N*-methylamino)][4′-(*N*′,*N*′-dimethylamino)][4″-(*N*″-methylamino)]triphenylmethanol	23.93	390.08	344.13	250.0
G′	ED-D−TPM	[4-(*N*-ethyl-*N*,*N*-dimethylamino)][4′-(*N*′,*N*′-dimethylamino)][4″-(amino)]triphenylmethanol	23.77	390.08	344.14; 255.08	251.2
H′	ED-MM−TPM	[4-(*N*-ethyl-*N*,*N*-dimethylamino)][4′-(*N*′-methylamino)][4″-(*N*″-methylamino)]triphenylmethanol	23.46	390.07	344.15; 255.09	240.6
I′	D−DM−TPM	[4-(*N*,*N*-dimethylamino)][4′-(*N*′,*N*′-dimethylamino)][4″-(*N*″-methylamino)]triphenylmethanol	20.09	376.32	344.14; 268.92; 254.95	245.3
J′	E-DM−TPM	[4-(*N*-ethylamino)][4′-(*N*′,*N*′-dimethylamino)][4″-(*N*″-methylamino)]triphenylmethanol	19.04	376.19	344.14; 255.08	246.5
K′	EM-D−TPM	[4-(*N*-ethyl-*N*-methylamino)][4′-(*N*′,*N*′-dimethylamino)][4″-(amino)]triphenylmethanol	15.64	362.01	254.95; 227.02	241.8
L′	EM-MM−TPM	[4-(*N*-ethyl-*N*-methylamino)][4′-(*N*′-methylamino)][4″-(*N*″-methylamino)]triphenylmethanol	13.89	362.07	240.99; 212.74	245.3
a	DDBP	4-(*N*,*N*-dimethylamino)-4′-(*N*′,*N*′-dimethylamino)benzophenone	44.30	269.04	147.89	365.5
b	DMBP	4-(*N*,*N*-dimethylamino)-4′-(*N*′-methylamino)benzophenone	35.45	255.01	268.98; 133.86	362.1
c	MMBP	4-(*N*-methylamino)-4′-(*N*′-methylamino)benzophenone	25.62	240.98	224.06	361.2
d	DBP	4-(*N*,*N*-dimethylamino)-4′-aminobenzophenone	23.12	241.06	252.96	344.2
a′	ED-DBP	4-(*N*-ethyl-*N*,*N*-dimethylamino)-4′-(*N*′,*N*′-dimethylamino)benzophenone	26.60	297.15	223.93; 175.93; 147.93	372.8
b′	ED-MBP	4-(*N*-ethyl-*N*,*N*-dimethylamino)-4′-(*N*′-methylamino)benzophenone	22.59	283.14	253.09	364.3
c′	EM-DBP	4-(*N*-ethyl-*N*-methylamino)-4′-(*N*′,*N*′-dimethylamino)benzophenone	21.41	283.04	253.09; 209.91	361.3
d′	E-DBP	4-(*N*-ethylamino)-4′-(*N*′,*N*′-dimethylamino) benzophenone	17.78	269.09		345.4
e′	ED-BP	4-(*N*-ethyl-*N*,*N*-dimethylamino)-4′-(amino)benzophenone	16.25	269.05	222.97	328.6
α	DAP	4-(*N*,*N*-dimethylamino)phenol	39.20	N/A		296.4
β	MAP	4-(*N*-methylamino)phenol	30.47	N/A		289.2
γ	AP	4-aminophenol	9.28	N/A		280.9
α′	EDAP	4-(*N*-ethyl-*N*,*N*-dimethylamino)phenol	40.19	166.21		297.2
β′	EMAP	4-(*N*-ethyl-*N*-methylamino)phenol	33.71	151.97		289.2
γ′	EAP	4-(*N*-ethylamino)phenol	13.41	N/A		288.1

no)benzophenone. The retention times and absorption spectra are identical.

(3) The third family was marked in the chromatogram and is illustrated in Figure 3c, recorded at 300 nm. The absorption spectra of each intermediate in the ultraviolet spectral region around 300 nm are depicted in the Supporting Information (see Figure 4, Supporting Information) corresponding to the peaks **α**−***γ*** and **α′**−***γ′*** in Figure 3c. The *N*-dealkylation of the DAP (EDAP), produced by cleavage of the CV (CB), has the wavelength position of its major absorption band moved toward the blue region, λ_{max}, **α**, 296.4 nm; ***β***, 289.2 nm; ***γ***, 280.9 nm (**α′**, 297.2 nm; ***β′***, 289.2 nm; ***γ′***,

SCHEME 1 . Proposed Photocatalytic Degradation Pathway of CV in Suspension of TiO_2 Irradiated by UV

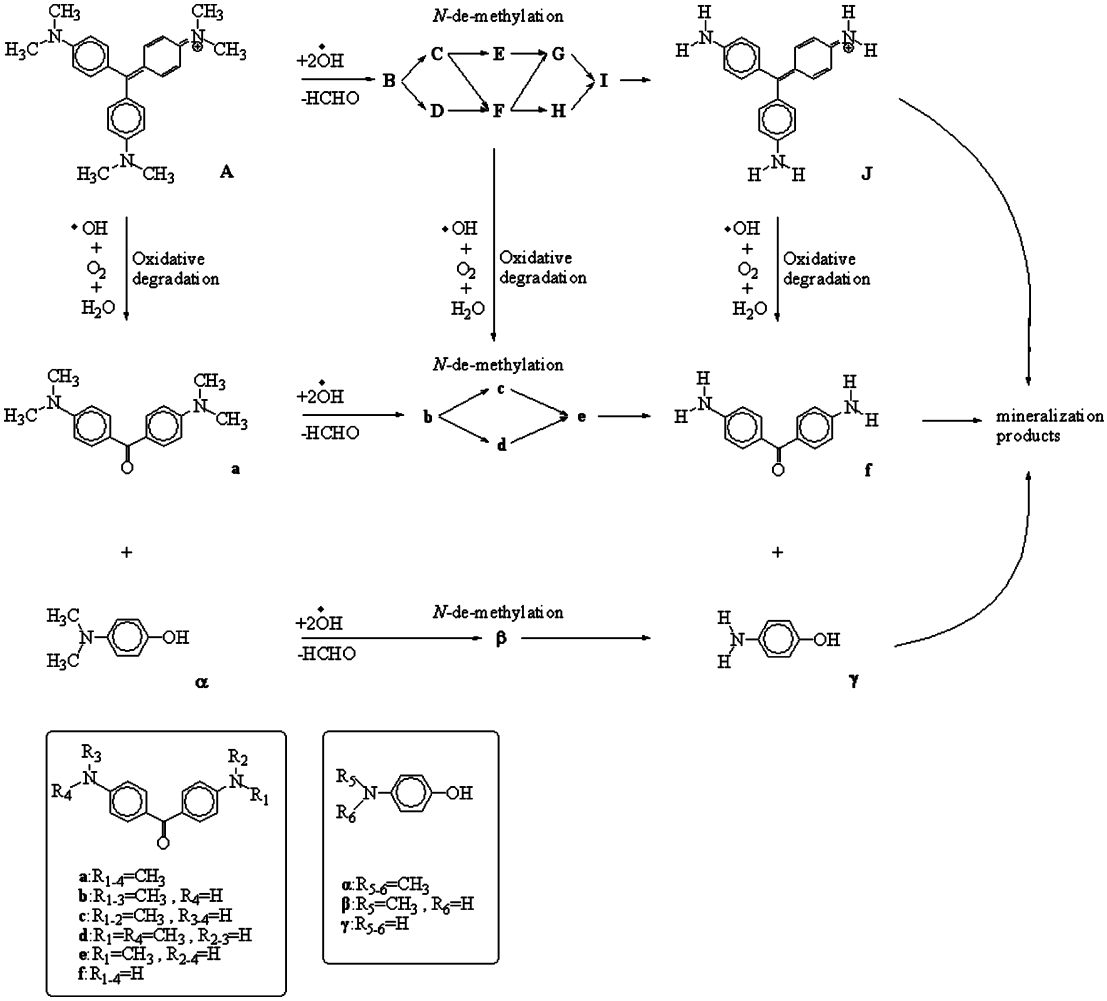

288.1 nm). The proposed intermediates (β, γ) have been compared with standard materials of 4-(*N*-dimethylamino)-phenol and 4-aminophenol. The retention times and absorption spectra are identical.

(4) The fourth family was marked in the chromatogram and is illustrated in Figure 3d, recorded at 250 nm. The absorption spectra of each intermediate in the visible and ultraviolet spectral region around 250 nm are depicted in the Supporting Information (see Figure 4, Supporting Information) corresponding to the peaks **A′**−**K′** in Figure 3d. The *N*-de-alkylation of the CB has the wavelength position of its major absorption band moved toward the blue region, λ_{max}, **A′**, 259.5 nm; **B′**, 254.8 nm; **C′**, 253.6 nm; **D′**, 248.9 nm; **E′**, 251.2 nm; F′, 250.0 nm; **G′**, 251.2 nm; **H′**, 240.6 nm; **I′**, 245.3 nm; **J′**, 246.5 nm; **K′**, 241.8 nm; **L′**, 245.3 nm. The cationic MG dye molecules are converted into the colorless CB, which is tertiary alcohol, by OH^-. The tertiary alcohol is colorless, with a peak absorbance at 254 nm (*22*). The data we observed above can be seen more clearly in Table 1.

3.6.2. Mass Spectra of the Intermediates. The photodegraded intermediates were further identified using the HPLC-ESI-MS techniques. The total ion chromatogram is illustrated in Figure 3e. The molecular ion peaks appeared in the acid forms of the intermediates. The relevant mass spectra of partial intermediates are illustrated in the Supporting Information (see Figure 5, Supporting Information). The results of mass spectral analysis confirmed that the component A, m/z = 372.13, is CV. The other components are **B**, m/z = 358.17; **C**, m/z = 344.21; **D**, m/z = 344.14; **E**, m/z = 330.11; **F**, m/z = 330.11; **G**, m/z = 316.09; **H**, m/z = 316.15; **I**, m/z = 302.25; **A′**, m/z = 418.27, is CB; **B′**, m/z = 404.18; **C′**, m/z = 404.15; **D′**, m/z = 390.09; **E′**, m/z = 390.09; **F′**, m/z = 390.08; **G′**, m/z = 390.08; **H′**, m/z = 390.07; **I′**, m/z = 376.32; **J′**, m/z = 376.19; **K′**, m/z = 362.01; **L′**, m/z = 362.07; **a**, m/z = 269.04; **b**, m/z = 255.01; **c**, m/z = 240.98; **d**, m/z = 241.06; **a′**, m/z = 297.15; **b′**, m/z = 283.14; **c′**, m/z = 283.04; **d′**, m/z = 269.09; **e′**, m/z = 269.05; **α′**, m/z = 166.21; **β′**, m/z = 151.97. Results of HPLC-ESI mass spectra are summarized in Table 1.

3.6.3. Separation and Identification of Isomer. In the first family, the absorption maxima of intermediates **D** (580.7 nm), **F** (568.5 nm), and **H** (561.2 nm) occur at longer wavelengths than those of intermediates **C** (573.4 nm), **E** (567.5 nm), **G** (555.0 nm), respectively. These species correspond to the intermediates that possess from two to four methyl groups relative to the CV dye and are correlative with three pairs of isomeric molecules. One of these isomers, DMMPR, is formed by removal of a methyl group from two different sides of the CV molecule while the other isomer in this pair, DDPR, is produced by removal of two methyl groups from the same side of the CV structure. The other pair of isomers is formed by removal of different methyl group. Considering that the polarity of the DDPR, DMPR, DPR, and DBP species exceed that of the DMMPR, MMMPR, MMPR, and MMBP intermediates, we expected the latter to be eluted after the DDPR, DMPR, DPR, and DBP species. Additionally, to the extent that two *N*-methyl groups are stronger auxochromic moieties than are the *N*,*N*-dimethyl or amino groups, the maximal absorption of the DDPR, DMPR, DPR, and DBP intermediates was anticipated to occur at wavelengths shorter than the

SCHEME 2 . Proposed Photocatalytic Degradation Pathway of CB in Suspension of TiO_2 Irradiated by UV

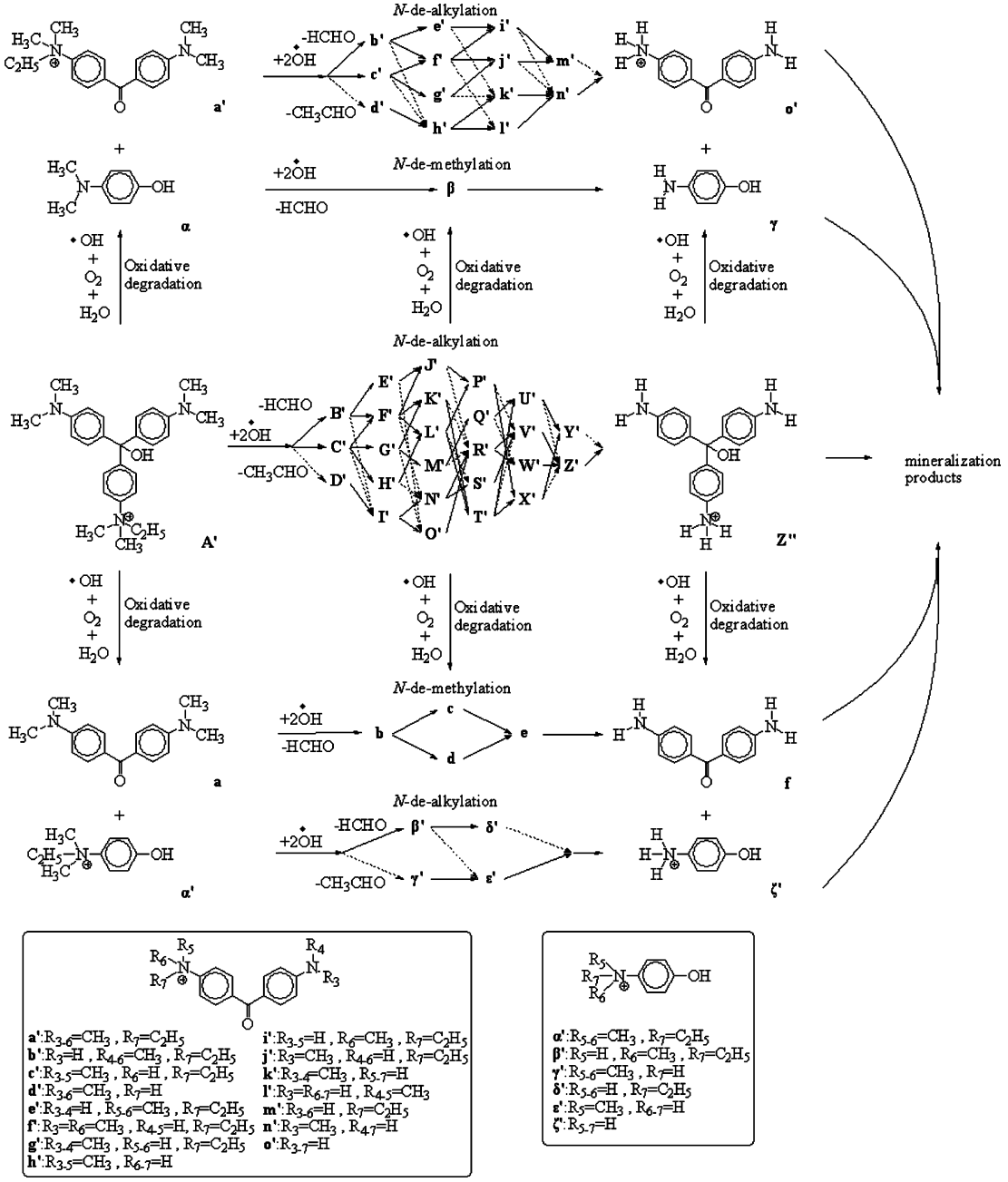

band position of the DMMPR, MMMPR, MMPR, and MMBP species. There is a similar situation in the other family. The following results and the proposed mechanism support this argument.

3.7. Degradation Mechanisms of MG. The MG dye dissolves to alkaline solution when the pH value is too high (pH 9). The cationic MG dye molecules are converted into the colorless carbinol base (CB; triarylmethanol), which is tertiary alcohol, by hydroxide anion. Additionally, the *N*-ethyl-*N*,*N*-dimethylammonium group of dye molecule is attacked by hydroxide anion to produce CV dye and ethanol (see Scheme 3, Supporting Information). The absorbance of the CV solution was measured at the absorption peak (580 nm) and compared with the calibration curve obtained by measurement of the absorbance of the standard aqueous solution. The mol ratio of CV/CB is 0.41. Then, CV and CB are degraded by the photocatalyst, TiO_2.

3.7.1. Photodegradation Mechanisms of CV. 3.7.1.1 *N*-de-methylation of CV.

The relative distribution of all of the intermediates obtained is illustrated in the Supporting Information (see **Figure 6**a, Supporting Information). To minimize errors, the relative intensities were recorded at the maximum absorption wavelength for each intermediate, although a quantitative determination of all of the photogenerated intermediates was not achieved, owing to the lack of appropriate molar extinction coefficients for them and to unavailable reference standards. The distributions of all of the *N*-de-methylated intermediates are relative to the initial concentration of CV. Nonetheless, we clearly observed the changes in the distribution of each intermediate during the photodegradation of CV. The successive appearance of the maximum of each intermediate indicates that the *N*-de-methylation of CV is a stepwise photochemical process. The possible degradation pathway is presented in Scheme 1. All the intermediates identified in the study were also identified in a previous study of the CV/TiO_2 system (*26*).

Under UV irradiation, most of the •OH radicals are generated directly from the reaction between the holes and surface-adsorbed H_2O or OH^- (*6*, *7*). The *N*-de-methylation of the CV dye occurs mostly through attack by the •OH species on the *N*,*N*-dimethyl portion of CV. The *N*-mono-de-methylated intermediate (DDMPR) was clearly observed (curve **B**) to reach its maximum concentration after a 4 h irradiation period. The other *N*-methylated intermediates, DMMPR, DDPR, DMMPR, DDPR, MMMPR, DMPR, MMPR, and DPR, were clearly observed (curves **E**−**I**) to reach their maximum concentrations after 4 h, 8 h, 8 h, 8 h, 12 h, 12 h, and 16 h irradiation periods, respectively. The successive appearance of the maximal quantity of each intermediate indicates that the *N*-de-methylation of CV is a stepwise photochemical process. CV gets near the negatively charged TiO_2 particle surface via the positive dimethylamine group. The results discussed above can be seen more clearly from Scheme 1.

3.7.1.2. Oxidative Degradation of the CV. The oxidative degradation of the CV dye occurs mostly through attack by the •OH species on the central carbon portion of CV and produces DDBP and DAP. The evolutions of the initial dye concentration and of the identified intermediates were followed as a function of irradiation time. The result is displayed in the Supporting Information (see **Figure 6**b, Supporting Information). The oxidative degradation intermediates, DDBP and DAP, were clearly observed (curve **a** and **α**) to reach their maximum concentrations at the same time after a 4 h irradiation period. The *N*-mono-de-methylated intermediates DMBP and MAP were clearly observed (curve **b** and ***β***) to reach their maximum concentrations at the same time after an 8 h irradiation period. The *N*-di-de-methylated intermediates MMBP, DBP, and AP were clearly observed (curves **c**−**d** and ***γ***) to reach their maximum concentrations after a 12 h irradiation period. The concentration of the other *N*-methylated intermediates may be under the detectable limit. CV is adsorbed on the TiO_2 particle surface via a conjugated structure, with the major photo-oxidation products being DDBP, DAP, their *N*-de-methylated products. The results we discussed above can be seen more clearly from Scheme 1.

3.7.2. Photodegradation Mechanisms of CB. 3.7.2.1. N-de-alkylation of CB. The relative distribution of all of the intermediates obtained is illustrated in the Supporting Information (see Figure 6c, Supporting Information). The distributions of all of the *N*-de-alkylated intermediates are relative to the initial concentration of CB. Nonetheless, we clearly observed the changes in the distribution of each intermediate during the photodegradation of CB. The *N*-de-alkylation of the CB occurs mostly through attack by the •OH species on the *N*,*N*-dimethyl group or *N*,*N*-dimethyl-*N*-ethyl group of CB. The *N*-mono-de-alkylated intermediate (ED-DM-TPM, EM-DD-TPM, D-DD-TPM) was clearly observed (curves **B′**, **C′**, **D′**) to reach its maximum concentration at the same time after a 4 h irradiation period. The other *N*-ethylated intermediates, **E′**−**K′**, were clearly observed (curves **E′**−**K′**) to reach their maximum concentrations after 8 h, 8 h, 8 h, 8 h, 8 h,12 h, and 12 h irradiation periods, respectively. The concentrations of the other de-alkylated products may be too low to be examined by HPLC-PDA-ESI-MS. The successive appearance of the maximal quantity of each intermediate indicates that the *N*-de-ethylation of CB is a stepwise photochemical process. The results discussed above can be seen more clearly from Scheme 2.

3.7.2.2. Oxidative Degradation of the CB. The oxidative degradation of the CB dye occurs mostly through attack by the •OH species on the central carbon portion of CB and produces two sets intermediates, DDBP and EDAP, and ED-DBP and DAP, under basic aqueous conditions. The evolutions of the initial dye concentration and of the identified intermediates were followed as a function of irradiation time. The oxidative degradation of two sets of intermediates was clearly observed (see **Figure 6**b, curves **a**, **α**, **a′** and **α′**, Supporting Information) to reach their maximum concentrations at the same time after a 4 h irradiation period. The other oxidative intermediates were clearly observed (curves **b**−**d**, ***β***−***γ***; **b′**−**e′** and ***β′***−***γ′***) to reach their maximum concentrations after 8, 12, 16, and 20 h irradiation periods, respectively. The results we discussed above can be seen more clearly from Scheme 2.

According to earlier reports (*27*−*30*), the *N*-de-alkylation processes are preceded by the formation of a nitrogen-centered radical while destruction of dye chromophore structures is preceded by the generation of a carbon-centered radical. Consistent with this, degradation of CV and CB must occur via two different photooxidation pathways (destruction of the structure and *N*-de-alkylation) due to formation of different radicals (either a carbon-centered or nitrogen-centered radical). There is no doubt that the •OH attack on the dye yields a dye cationic radical. After this step, the cationic radical $Dye^{\bullet+}$ can undergo hydrolysis and/or use various deprotonation pathways, which in turn are determined by the different adsorption modes of CV and CB on the TiO_2 particle surface.

Acknowledgments

This research was supported by the National Science Council of the Republic of China (NSC 95-2113-M-438-001).

Supporting Information Available

Adsorption spectra of the photodegraded intermediates, ESI mass spectra of partial intermediates, variation in the relative distribution of the *N*-de-methylated products, and the proposed degradation pathway of MG under basic solution. This material is available free of charge via the Internet at http://pubs.acs.org.

Literature Cited

(1) Linsebigler, A. L.; Lu, G. Q.; Yates, J. T. Photocatalysis on TiO_2 surfaces: principles, mechanisms, and selected results. *Chem. Rev.* **1995**, *95* (3), 735−758.

(2) Hoffman, M. R.; Martin, S. T.; Choi, W.; Bahnemann, W. Environmental applications of semiconductor photocatalysis. *Chem. Rev.* **1995**, *95* (1), 69−96.

(3) Watanabe, N.; Horikoshi, S.; Kawasaki, A.; Hidaka, H.; Serpone, N. Formation of refractory ring-expanded triazine intermediates during the photocatalyzed mineralization of the endocrine disruptor amitrole and related triazole derivatives at UV-irradiated TiO_2/H_2O interfaces. *Environ. Sci. Technol.* **2005**, *39* (7), 2320−2326.

(4) Bouzaida, I.; Ferronato, C.; Chovelon, J. M.; Rammah, M. E.; Herrmann, J. M. Heterogeneous photocatalytic degradation of the anthraquinonic dye, Acid Blue 25 (AB25): a kinetic approach. *J. Photochem. Photobiol. A: Chem.* **2004**, *168* (1), 23−30.

(5) Lu, P.; Wu, F.; Deng, N. S. Enhancement of TiO_2 photocatalytic redox ability by β-cyclodextrin in suspended solutions. *Appl. Catal., B* **2004**, *53* (2), 87−93.

(6) Nakamura, R.; Nakato, Y. Primary intermediates of oxygen photoevolution reaction on TiO_2 (rutile) particles, revealed by in situ FTIR adsorption and photoluminescence measurements. *J. Am. Chem. Soc.* **2004**, *126* (4), 1290−1298.

(7) Murakami, Y.; Kenji, E.; Nosaka, A. Y.; Nosaka, Y. Direct detection of radicals diffused to the gas phase from the UV-irradiated photocatalytic TiO_2 surfaces by means of laser-induced fluorescence spectroscopy. *J. Phys. Chem. B* **2006**, *110* (34), 16808−16811.

(8) Konstantinou, I. K.; Albanis, T. A. TiO_2-assisted photocatalytic degradation of azo dyes in aqueous solution: kinetic and mechanistic investigations: A review. *Appl. Catal., B* **2004**, *49* (1), 1−14.

(9) Ishibashi, K.; Fujishima, A.; Watanabe, T.; Hashimoto, K. Generation and deactivation processes of superoxide formed on TiO_2 film illuminated by very weak UV light in air or water. *J. Phys. Chem. B.* **2000**, *104* (20), 4934−4938.

(10) Tatsuma, T.; Tachibana, S.; Fujishima, A. Remote Oxidation of Organic Compounds by UV-Irradiated TiO_2 via the Gas Phase. *J. Phys. Chem. B* **2001**, *105* (29), 6987−6992.
(11) Tachikawa, T.; Takai, Y.; Tojo, S.; Fujitsuka, M.; Majima, T. Probing the surface adsorption and photocatalytic degradation of catechols on TiO_2 by solid-state NMR spectroscopy. *Langmuir* **2006**, *22* (3), 893−896.
(12) Nosaka, A. Y.; Nishino, J.; Fujiwara, T.; Ikegami, T.; Yagi, H.; Akutsu, H.; Nosaka, Y. Effects of thermal treatments on the recovery of adsorbed water and photocatalytic activities of TiO_2 photocatalytic systems. *J. Phys. Chem. B* **2006**, *110* (16), 8380−8385.
(13) Duxbury, D. F. The photochemistry and photophysics of triphenylmethane dyes in solid and liquid media. *Chem. Rev.* **1993**, *93* (1), 381−433.
(14) Inoue, T.; Kikuchi, K.; Hirose, K.; Iiono, M.; Nagano, T. Small molecule-based laser inactivation of inositol 1, 4, 5-triphosphate receptor. *Chem. Biol.* **2001**, *8* (1), 9−15.
(15) Green, F. J. *The Sigma-Aldrih Handbook of Stains, Dyes, and Indicators*; Aldrich Chemical: Milwaukee, WI, **1990**.
(16) Geethakrishnan, T.; Palanisamy, P. K. Degenerate four-wave mixing experiments in methyl green dye-doped gelatin film. *Optik* **2006**, *117* (6), 282−286.
(17) Melnick, J.; Pickering, M. The mechanism of the drug induced partial displacement of methyl green from DNA. *Biochem. Int.* **1988**, *16* (1), 69−75.
(18) Bonnett, R.; Martinez, G. Photobleaching of sensitisers used in photodynamic therapy. *Tetrahedron* **2001**, *57* (47), 9513−9547.
(19) Cho, B. P.; Yang, T.; Blankenship, L. R.; Moody, J. D.; Churchwell, M.; Bebland, F. A.; Culp, S. J. Synthesis and characterization of *N*-de-methylated metabolites of malachite green and leuco-malachite green. *Chem. Res. Toxicol.* **2003**, *16* (3), 285−294.
(20) Zhao, J.; Wu, T.; Wu, K.; Oikawa, K.; Hidaka, H.; Serpone, N. Photoassisted degradation of dye pollutants. 3. Degradation of the cationic dye rhodamine B in aqueous anionic surfactant/TiO_2 dispersions under visible light irradiation: evidence for the need of substrate adsorption on TiO_2 particles. *Environ. Sci. Technol.* **1998**, *32* (16), 2394−2400.
(21) Wu, T.; Liu, G.; Zhao, J.C.; Hidaka, H.; Serpone, N. Photoassisted degradation of dye pollutants. V. Self-photosensitized oxidative transformation of rhodamine B under visible light irradiation in aqueous TiO_2 dispersions. *J. Phys. Chem. B* **1998**, *102*(30), 5845−5851.
(22) Abbruzzetti, S.; Carcelli, M.; Pelagatti, P.; Rominga, D.; Viappiani, C. Photoinduced alkaline pH-jump on the nanosecond time scale. *Chem. Phys. Lett.* **2001**, *344* (3−4), 387−394.
(23) Liu, G.; Li, X.; Zhao, J.; Hidaka, H.; Serpone, N. Photooxidation pathway of sulforhodamine-B. Dependence on the adsorption mode on TiO_2 exposed to visible light radiation. *Environ. Sci. Technol.* **2000**, *34*(18), 3982−3990.
(24) Liu, G.; Zhao, J. Photocatalytic degradation of dye sulforhodamine B: a comparative study of photocatalysis with photosensization. *New J. Chem.* **2000**, *24*(2), 411−417.
(25) Boehm, H. P. Acidic and basic properties of hydroxylated metal oxide surfaces. *Discuss. Faraday Soc.* **1971**, *52* (2), 264−276.
(26) Chen, C. C.; Fan, H. J.; Jang, C. Y.; Jan, J. L.; Lin, H. D.; Lu, C. S. Photooxidative N-de-methylation of crystal violet dye in aqueous nano-TiO_2 dispersions under visible light irradiation. *J. Photochem. Photobiol., A* **2006**, *184* (1−2), 147−154.
(27) Shaefer, F. C.; Zimmermann, W. D. Dye-sensitized photochemical autoxidation of aliphatic amines in non-aqueous media. *J. Org. Chem.* **1970**, *35* (7), 2165−2174.
(28) Galliani, G.; Rindone, B.; Scolastico, C. Selective de-methylation in the oxidation of arylalkylmethylamines with metal acetates. *Tetrahedron Lett.* **1975**, *16* (15), 1285−1288.
(29) Lewis, G. N.; Lipkin, D.; Nagel, T. T. The Light Absorption and Fluorescence of Triarylmethyl Free Radicals. *J. Am. Chem. Soc.* **1944**, *66* (9), 1579−1583.
(30) Manring, L. E.; Peters, K. S. Picosecond dynamics of the photodissociation of triarylmethanes. *J. Phys. Chem.* **1984**, *88* (16), 3516−3520.

Received for review October 14, 2006. Revised manuscript received March 20, 2007. Accepted April 3, 2007.

ES062465G